Fatigue monitoring of climbing ropes

(Article begins on next page)

23 April 2024

Fatigue monitoring of climbing ropes

Renato Galluzzi, Stefano Feraco, Enrico C Zenerino, Andrea Tonoli, Angelo Bonfitto and Shailesh Hegde

Abstract

Safety improvements in mountaineering gear have enabled the increasing popularity of rock climbing as a sport. Both amateurs and experts want to know the condition of their equipment with a high degree of reliability. For climbing ropes, diagnostics are only carried out qualitatively by visual inspection. The assessment is left to the personal judgment of the user, thus leaving considerable margins of uncertainty on the rope's condition. To address this shortcoming, this paper explores the possibility of estimating fatigue damage from the impact force on the rope. This value is estimated from the measurements of the climber's acceleration using a wearable device. Then, force data are correlated to the fatigue characteristic of the rope. In this study, three ropes were used by professional climbers through different routes. After this field conditioning, the ropes were tested following the UIAA standard and compared to a control rope. The results show that the proposed method can estimate the rope cumulative damage, but it relies on the accuracy of the damage model. In particular, the parameter describing the contact between the rope and the runner is important for a correct estimate.

Prepared using *sagej.cls* *[Version: 2017/01/17 v1.20]*

Introduction

Climbing has recently gained popularity as both an indoor and outdoor sport.[1] A decisive factor of this diffusion can be attributed to the safety improvements in the rigging equipment in the last two decades. The user's confidence in the reliability of the safety chain when in sport climbing routes allows him/her to take the risk of a fall, knowing that the risk of injury will be minimized in the vast majority of the cases. Furthermore, mountaineering equipment safety standards have become more stringent.[2–4] In this evolution, technology improvements have played a substantial role in the sport's popularity.

In general, climbers take conservative safety measures to preserve the health of their mountaineering equipment. However, a failure in this context may still lead to severe consequences for the user. Therefore, many researchers have investigated the behavior of climbing gear in terms of safety.[5] Studies on the strength and failure of anchor points have been conducted.[6] Blair *et al.* have analyzed the fatigue failure in D-shaped carabiners.[7] The failure of the quickdraw, consisting of carabiners and sling, has also been evaluated.[8] Other works demonstrate that the change in rope paths has a relevant effect on the belay point.[9] In addition, Manin *et al.* model the climber fall arrest dynamics[10] and present a method to characterize the belay device and analyze the impact load.[11]

The climbing rope is one of the most important parts of the climber's safety equipment, since it is the only anchor point between the climber harness and the rock. Ropes present a kernmantle construction type with nylon fibers that constitute the core and a sheath envelope that covers them. The visual inspection of the sheath can reveal the rope's condition to a limited extent. This qualitative evaluation is useful when evident signs of deterioration are present, such as superficial abrasion.

Much of the scientific literature in the mountaineering field has investigated the climbing rope. Some of these works focus on the experimental validation through dynamic loading and fall transients.[12,13] Other efforts have dealt with exposition to environmental factors, such as moisture.[14,15] Studies regarding rope material aging have also been conducted.[16]

Diverse attempts have been devoted to a proper understanding of the lifespan of ropes. In the marine industry, Mandell[17] and Kenney et al.[18] characterized the rope load-cycle behavior and studied different effects, such as abrasion and frequency. Beltran and Williamson developed a computational model to

Department of Mechanical and Aerospace Engineering, Politecnico di Torino, Italy

Corresponding author:
Renato Galluzzi, Department of Mechanical and Aerospace Engineering, Politecnico di Torino, Corso Duca degli Abruzzi 24, 10129 Turin, Italy.
Email: renato.galluzzi@polito.it

predict the response of synthetic-fiber ropes under both monotonic and cyclic loads.[19] Johnson and Klonowsky studied the role of abrasive particles on the lifespan of nylon ropes.[20] In a more general effort, Pavier conducted experimental tests to build a fatigue characteristic for climbing ropes.[21]

Recently, Leuthäusser has dealt with the elongation dynamics of the climbing rope when under heavy load.[22] More importantly, he has studied the mechanisms that intervene in the fracture process of climbing ropes.[23] He determined a useful load-cycle characteristic validated with more than twenty commercial climbing rope specimens of different types and arrangements (single, twin and half). This information opens the possibility of estimating the residual life of a rope by knowing the load history acting upon it. Interestingly, a real-time estimate of the rope damage after the fall event would give the climber a better insight on the health status of the equipment, thus going beyond the reliability limitations of visual inspection. The availability of more information about the remaining useful life of the rope can boost the climber's confidence in the adopted equipment.

This scenario highlights the advances in safety equipment and ropes in particular, both from technology and methodology standpoints. In this context, the present paper aims to analyze the feasibility of damage estimation in climbing ropes through activity tracking. Previous works have shown that it is possible to detect climbing falls with a reasonable level of accuracy by means of wearable data logging devices equipped with off-the-shelf motion sensors.[24,25] A further simple enhancement of the fall detection algorithm would allow for the extraction of the acceleration peak at the instant of impact. This information is useful to calculate the force amplitude acting on the rope; a subsequent correlation of this information to a fatigue curve could lead to an estimate of the rope damage. Despite the growing popularity of wearable devices for monitoring athletes' performance, no studies or applications regarding fatigue monitoring of climbing ropes are available.

This study presents the calculation of cumulative damage on three ropes used by professional climbers going through mixed difficulty climbing routes. A subsequent verification of the technique was carried out by estimating the residual life of the ropes through destructive tests following the UIAA standard.[26]

Method

The present research aims to monitor the fatigue of climbing ropes. For this purpose, users were equipped with a wearable device able to detect climbing falls and estimate the impact force (i.e. the maximum force exerted to the rope during a fall event). As presented in previous works, the combination of triaxial acceleration and altimetry measurements allows the detection of climbing falls through different post-processing algorithms with the possibility of working in real time.[24,25] Assuming the implementation of such techniques, one can find the acceleration peak due to a fall impact. Therefore, the force acting on

the rope in a fall event is given by Eq. (1)

$$\hat{F} = m \left| \vec{a} \right|, \tag{1}$$

where m is the mass of the climber and $\vec{a}$ is the measured acceleration vector at the instant of impact.

To assess the rope fatigue, these force impact events must be associated to a force-cycle curve such as those used in material science. Characterizations like those introduced by Pavier[21] or Leuthäusser[23] are useful for this purpose.

The validation of the method requires gathering the data from different climbers. Their recorded activity logs were merged and post-processed to identify the fall events and extract the impact acceleration peaks, which were used to determine the impact forces using Eq. (1). One can predict the damage of the rope by associating these data with a force-cycle characteristic through a suitable damage rule.

For safety reasons, the ropes were partially utilized and then tested in a laboratory to quantify their residual lifespan. After field conditioning sessions, the ropes were segmented and validated according to the UIAA standard[26] to assess the damage prediction.

Fatigue model

For the purposes of this research, Leuthäusser's phenomenological approach[23] is a valid, useful tool. He determined a model able to reproduce the load-cycle characteristic of more than twenty commercial climbing ropes. The model requires the identification of a limited number of parameters. This generality is of great importance to the present work. It facilitates the implementation of a reliable experimentally-validated fatigue model from which the proposed method can estimate the rope damage.

Leuthäusser's approach subdivides the rope fracture process into two mechanisms: plastic deformation and local damage of the rope corresponding to the contact zone of the runner.

When stretched, the rope is subject to an elastic force as shown in Eq. (2)

$$F = a_1 \frac{x}{L^{\mathrm{e}}} + a_3 \left(\frac{x}{L^{\mathrm{e}}} \right)^3 \tag{2}$$

where x is the axial length coordinate of the rope, L^{e} is its maximum possible elongation and a_1, a_3 are characteristic force coefficients. Hence, this force has a maximum value as shown in Eq. (3) at

$$F^{\mathrm{max}} = a_1 + a_3 \tag{3}$$

Similarly, the energy that the rope absorbs is given by the integral of F over the infinitesimal $\mathrm{d}x$, with a maximum strain energy value shown in Eq. (4)

$$U = \frac{L^{\mathrm{e}}}{2} \left(a_1 + \frac{a_3}{2} \right) \tag{4}$$

The relationship between energy and force variables can be also expressed in power law notation as shown in Eq. (5)

$$\left(\frac{\hat{F}}{F^{\mathrm{max}}} \right)^m \cong \left(\frac{U^{\mathrm{fall}}}{U} \right)^{\frac{m}{m+1}} \tag{5}$$

where $\hat{F}$ is the force exerted to the rope and U^{fall} is the energy stored after a fall event.

For practical values of coefficients a_1 and a_3, the following approximation in Eq. (6) holds:

$$\frac{\hat{F}}{F^{\mathrm{max}}} \cong \left(\frac{U^{\mathrm{fall}}}{U} \right)^{\frac{3}{4}} \tag{6}$$

When dealing with the fracture phenomenon, the plastic deformation can be attributed to a homogeneous relationship also present in the phenomenological Bingham model. It involves the impact stress $\hat{\sigma}$, the yield stress σ^{y} and a viscosity parameter η as shown in Eq. (7)

$$\varepsilon_n^{\mathrm{p}} = \frac{\hat{\sigma}_n - \sigma^{\mathrm{y}}}{\eta} \tag{7}$$

provided that $\hat{\sigma}_1 \geq \sigma^{\mathrm{y}}$ for the first event and $\hat{\sigma}_n \geq \hat{\sigma}_{n-1}$ for successive ones. This plasticity reduces the maximum possible elastic deformation as shown in Eq. (8)

$$L_{n+1}^{\mathrm{e}} = L_1^{\mathrm{e}} \left(1 - \varepsilon_n^{\mathrm{p}} \right) \tag{8}$$

and, because the maximum energy storage is proportional to L_n^{e}, the elastic energy content is ruled by Eq. (9)

$$U_{n+1}^{\mathrm{e}} = U \left(1 - \varepsilon_n^{\mathrm{p}} \right) \tag{9}$$

Equations (6) to (8) can be combined to describe the dynamics of the plastic strain under stress cycling of amplitude $\hat{\sigma}_1$ as shown in Eq. (10)

$$\varepsilon_{n+1}^{\mathrm{p}} = \frac{\hat{\sigma}_1}{\eta} \left(\frac{1}{1 - \varepsilon_n^{\mathrm{p}}} \right)^{\frac{3}{4}} - \frac{\sigma^{\mathrm{y}}}{\eta} \tag{10}$$

The outlined plastic behavior employs the yield stress as a threshold that activates a process. In the first fall, polymeric units that overcome σ^{y} cross an energy barrier and remain trapped in a new potential state after load release. In subsequent falls, the yield effect is increasingly smaller because more elastic units are trapped in the unfolded state. Macroscopically, this leads to a phenomenon called strain hardening. [23]

By converse, the localized damage on the contact area between the rope and the anchor point can be described by the Weibull failure probability as shown in Eq. (11)

$$P_{\mathrm{f}}(x) = 1 - \exp \left(-\mu \left(\frac{x}{L} \right)^{m\lambda} \right) \tag{11}$$

where $\mu = 0.09$ is a damage parameter inversely proportional to the anchor point radius and $\lambda = 2.5$ is a geometrical parameter from contact mechanics. These parameters were identified by Leuthäusser when fitting the behavior of more than twenty different ropes in UIAA tests.

The integration of both damage mechanisms yields to the critical number of falls which a rope can hold before it fails (falls to failure minus one) as shown in Eq. (12)

$$n^* = \left\lceil \frac{1}{\mu\lambda} \left(\left(\frac{U_n^{\mathrm{e}}}{U^{\mathrm{fall}}} \right)^{\frac{m\lambda}{m+1}} - 1 \right) \right\rceil \tag{12}$$

For the purely elastic case, $U_n^{\mathrm{e}} = U$. In addition, for a large number of fall events n, Eq. (13) holds true

$$1 - \mu\lambda \sum_{i=1}^{n} \left(\frac{U_i^{\mathrm{fall}}}{U} \right)^{\frac{m\lambda}{m+1}} \approx 0 \tag{13}$$

This expression allows one to establish the Palmgren-Miner rule for fatigue as shown in Eq. (14), where D_n is the cumulative damage after n events.

$$D_n = \sum_{i=1}^{n} d_i \tag{14}$$

The damage component due to the single ith fall event is shown in Eq. (15), when $D_n > 1$, the rope reaches the fracture condition.

$$d_i = \mu\lambda \left(\frac{\hat{F}_i}{F^{\max}} \right)^\lambda \tag{15}$$

The Palmgren-Miner approach is a linear damage rule with load-level and load-sequence independence. It assumes that the damage done by each stress repetition at a given level is equal, meaning that the first stress cycle at a uniform level is as damaging as the last. To account for plasticity, this rule must be modified by using dynamic Eqs. (9) and (10).

Assuming a constant probability (Eq. (11)), the standard deviation that describes the fluctuations in the obtained fatigue characteristic is given by Eq. (16)

$$\Sigma(n) = \mathrm{CV}^{\mathrm{Wb}}\sqrt{n^*} \tag{16}$$

where $\mathrm{CV}^{\mathrm{Wb}} = 0.4$ is the coefficient of variation of the Weibull distribution for $\lambda = 2.5$.

Fatigue behavior of the control rope

For test control purposes, a new Beal Joker Unicore 9.1 rope was segmented into three samples and tested following the UIAA guidelines.[26] One end of the specimen was fixed, while the other was attached to a falling mass of $80\ \mathrm{kg}$. The body of the rope slipped through a support runner with a fillet radius of $5\ \mathrm{mm}$. During the tests, the mass was dropped at a fall factor as shown in Eq. (17)

$$f = \frac{2h}{L} = 1.77 \tag{17}$$

with h being the distance fallen and L the length of the rope available to absorb the fall. Environment temperature and humidity were monitored to ensure compliance with the UIAA standard.

The test rig was equipped with a force transducer to measure the impact force for each run. The position of the falling mass was also recorded. These data were used to produce the force-deformation characteristic of the tested samples. To compute the deformation, the elongation variable x was normalized with respect to L_i^{e}. Then, the curves were fitted according to Eq. (2). Experimental and fit results for the three samples are shown in Fig. 1. This procedure helped to identify force coefficients a_1 and a_3.

The yield stress σ^{y} and the viscosity parameter η were obtained from the fatigue characterization of the control rope, whereas damage and geometrical parameters (μ and λ, respectively) were taken from
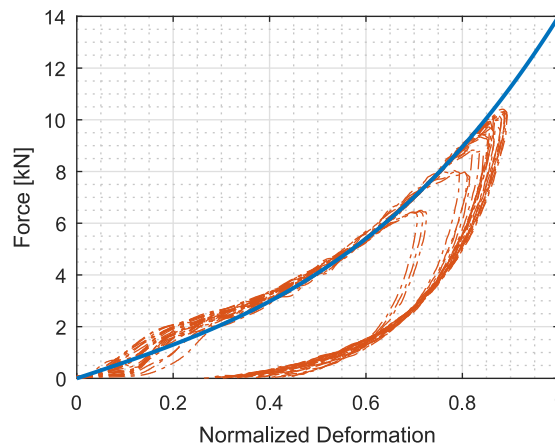
Figure 1. Force-deformation characteristic of a Beal Joker 9.1 climbing rope tested according to the UIAA standard for the present research. Experimental loops of three rope samples (dash-dot) are fitted according to Eq. (2) (solid).

Table 1. Beal Joker 9.1 rope parameters.

Description	Symbol	Value	Unit
First-degree force coefficient	a_1	6.2	kN
Third-degree force coefficient	a_3	7.8	kN
Yield stress	σ^{y}	95	MPa
Viscosity parameter	η	650	MPa
Damage parameter*	μ	0.09	–
Geometrical parameter*	λ	2.5	–

     * *fitted by Leuthäusser[23] for UIAA tests*

Leuthäusser's theory. Hence, the parameters listed in Table 1 were used to reproduce the force-cycle characteristic of the control rope, first for the purely elastic case and then including the plastic behavior, as outlined in the "Fatigue model" subsection. Both curves are illustrated in Fig. 2.

Afterwards, the force peak registered for each run was correlated to the obtained characteristic to compute its damage component.

Field conditioning of ropes

Three professional climbers were equipped with wearable data loggers and new Beal Joker Unicore 9.1 ropes from the same production batch as the control rope. For simplicity, they are identified by the number of their rope (1,2,3). These climbers ascended slab and overhang routes with mixed difficulty levels ranging from 6B to 8A+ in the French numerical grading system. It is expected that the end of
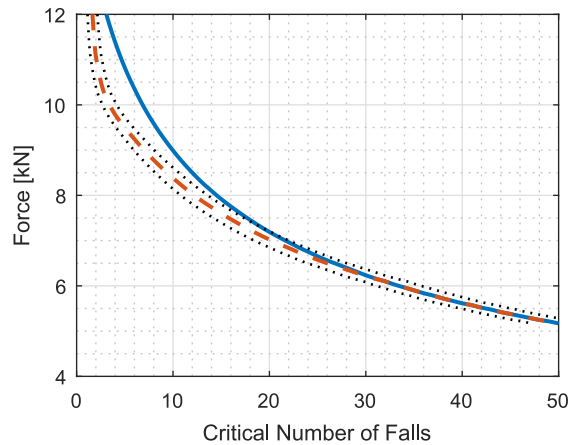
Figure 2. Force-cycle characteristic of a Beal Joker 9.1 climbing rope. The purely elastic curve (solid) is compared to the behavior that accounts for plasticity (dashed). According to Eq. (16), the standard deviation of the characteristic with plasticity is also displayed (dotted).

the rope attached to the climber is prone to greater wear due to usage. Hence, one end of each rope was labeled to anchor the user and ensure similar wear distributions among sessions.

The wearable devices were set to record the climbing activity from triaxial acceleration and altitude measurements sampled at 100 Hz. After the climbing sessions, time histories were extracted from the loggers and fed into a fall detection algorithm. This approach to identifying the climbing falls can be executed in real time if embedded into the data logger microcontroller, or it might be an offline post-processing routine. Details regarding this step have been investigated in the past by the authors.

In a first attempt, a Kalman filter was implemented to combine acceleration and altitude measurements.[24] By means of sensor fusion, this allowed for reconstructing the kinetic energy density as shown in Eq. (18)

$$E = \frac{v^2}{2} \tag{18}$$

where v is the velocity of the falling body. The fall event can be determined by simply applying a threshold to this quantity.

Recently, the authors also applied a pattern recognition neural network trained to detect the fall event from the same data set.[25] Because of its adaptive learning ability, this method does not require any fixed threshold on the studied variables.

A frequency characterization of the data logger[24] demonstrates that the device has a linear sensitivity behavior up to 15g, i.e. 10 kN considering a user of 68 kg. These measurements showed a relative
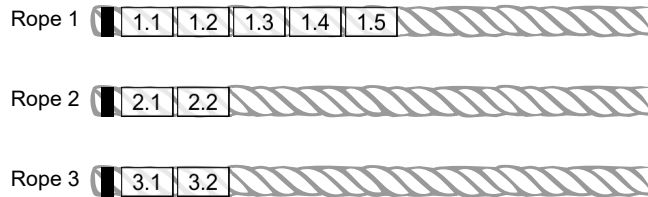
Figure 3. Rope segmentation for fatigue tests. The black stripe indicates the end attached to the user.

deviation lower than $\pm 3\%$ in the worst case. Furthermore, the attenuation at 100 Hz is -2.72 dB, which matches the desired bandwidth.

In practice, the acceleration measurement performed by the data logger might contain spurious components due to the climbing motion and interaction with the environment. These activity disturbances lead to slightly higher acceleration spikes that overestimate the actual impact force applied to the rope. Nevertheless, the acquired signal was kept unfiltered to provide a conservative estimate.

Once the fall events were identified, the acceleration peaks associated with those occurrences were extracted. Subsequently, the impact load on the rope was determined through Eq. (1). This result could be fed into Eq. (15) to estimate the rope damage.

The application of contact stresses and subsequent localized damage in the field may differ significantly from the stress and damage that occur in the UIAA drop tests. Consequently, different values of the damage parameter μ are also expected between these two conditions. Since single and cumulative damage terms are directly proportional to μ, they were prorated as d_i/μ and D_n/μ, respectively. A suitable μ parameter will be found in a subsequent UIAA test campaign using the field-conditioned ropes.

Fatigue behavior of field-conditioned ropes

The field conditioning was followed by an experimental characterization of the ropes according to UIAA to determine their residual life. As the control rope, the climbers' ropes were segmented into four-meter samples according to Fig. 3. For consistency, all the ropes present an age prior to the laboratory tests of approximately 300 days. The ropes were tested with the same fall factor as the control rope (1.77).

Results

Figure 4 illustrates both the cumulative damage and the impact force for the three control rope specimens. Since the attained forces go beyond 6 kN, plastic behavior must be taken into account.
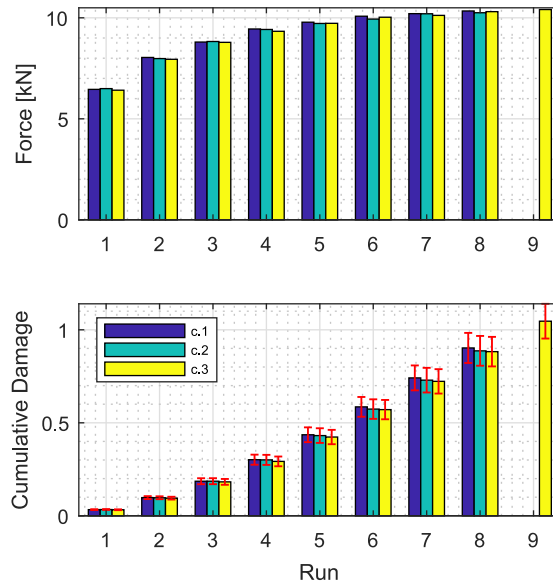
Figure 4. Measured impact force (top) and calculated cumulative damage (bottom) for three segments of the Beal Joker 9.1 control rope from UIAA tests. Data are plotted for $0 < n \leq n^*$. Failure occurs at $n = n^* + 1$. Cumulative damage error bars are also displayed.

The implemented model is able to reproduce the fatigue behavior for the three rope samples. For two of the rope samples, nine falls were necessary to reach a fracture condition ($n^* = 8$). The third sample required an additional run ($n^* = 9$). Impact force and cumulative damage present very similar trends among specimens.

Subsequently, Figs. 5 to 7 illustrate the results for the field conditioning of the three analyzed ropes. For display convenience, all the fall event data of a single climber are cut and merged into one plot, where acceleration, fall height and μ-normalized damage are presented as time histories.

From the measured acceleration peaks, one can notice that the impact forces do not exceed 4 kN and hence, the simpler, purely-elastic fatigue curve could be used to estimate the damage.

Finally, the knowledge of the load history from the test bench allows the computation of the cumulative damage on each segment, as seen in Fig. 8. The damage computed at n^* was adopted as the residual life of the segment. Ideally, the sum of the field damage and the residual life from UIAA tests should yield $D_n = 1$. This assumption allows the identification of a suitable value for μ in the field.

Table 2 reports relevant information from the complete experimental characterization. For each rope (Column 1), the μ-normalized cumulative damage was indicated from field conditioning (Column 2). After the rope segmentation (Column 3) and UIAA tests, the authors introduced the critical number of
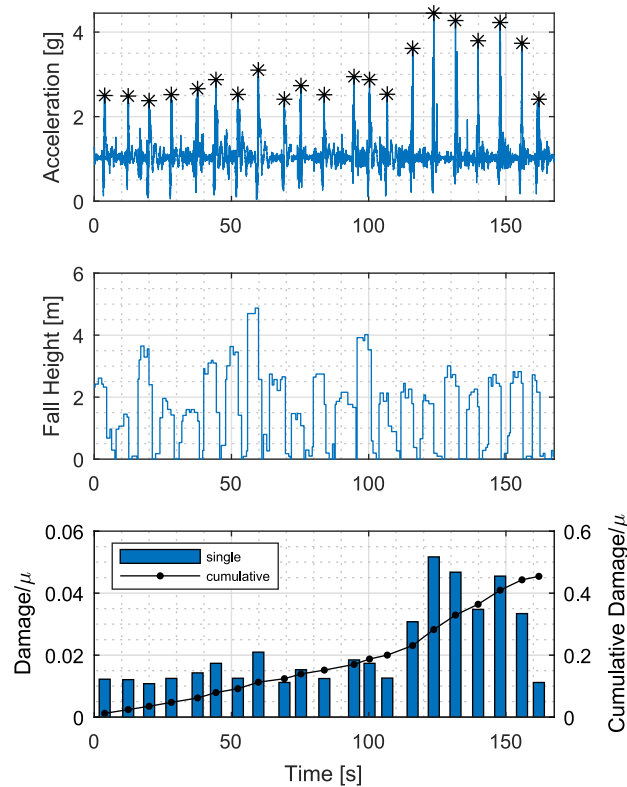
Figure 5. Rope 1 data. Top: acceleration magnitude (solid) and peaks (asterisk). Middle: fall height profile (solid). Bottom: single-event damage (bar) and cumulative damage (dot), both normalized with respect to μ.

falls n^* registered on the test bench for each rope sample (Column 4). The cumulative damage computed with n^* represents the residual life of each rope segment, as reported in Column 5. Finally, in Column 6, μ was estimated to match a total damage $D_n = 1$ when adding the field conditioning results and the residual life. It is worth noting that this new value of μ only affects the field test results; UIAA data use the value $\mu = 0.09$, as denoted by Leuthäusser.[23]

Discussion

As previously stated, the behavior of the control rope was used to tune the fatigue model in UIAA tests. The cumulative damages plotted in Fig. 4 confirm a successful tuning of the model.

During field conditioning (Figs. 5 to 7), most falls occurred at the end of a pitch, with the climber close to the final anchor point. Therefore, they are predominantly characterized by a fall factor below
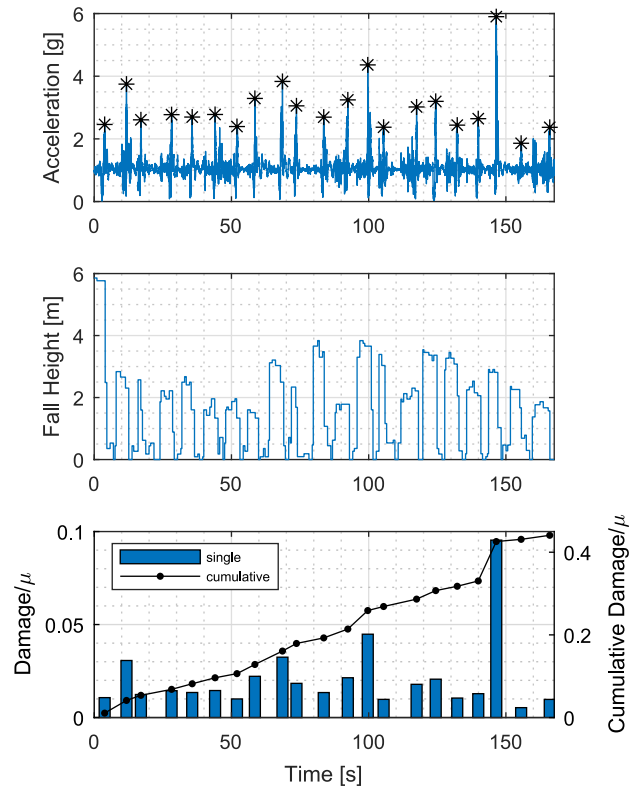
Figure 6. Rope 2 data. Top: acceleration magnitude (solid) and peaks (asterisk). Middle: fall height profile (solid). Bottom: single-event damage (bar) and cumulative damage (dot), both normalized with respect to μ.

Table 2. Fatigue characterization results.

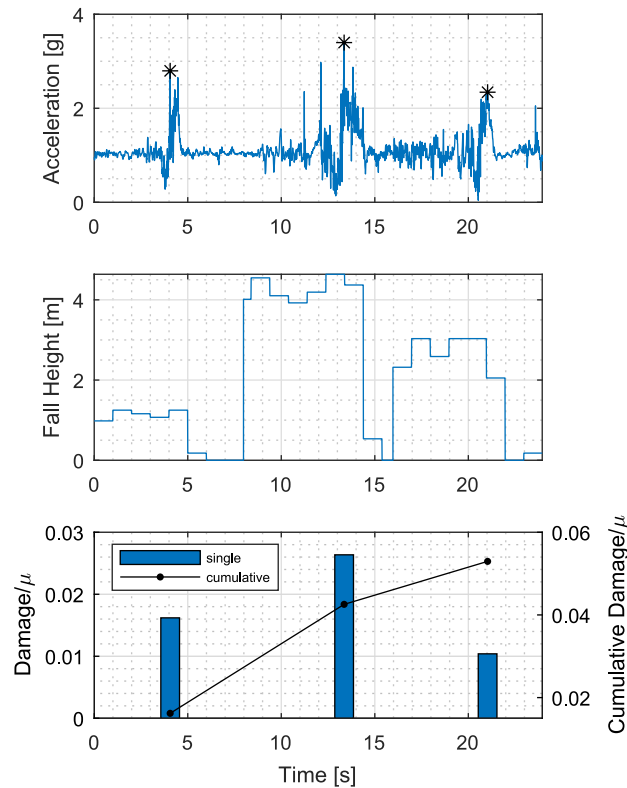| Rope	Cumulative damage/μ *field*	Segment	Critical number of falls $n^\star$ *UIAA tests*	Residual life *UIAA tests*	Required μ *field*
control	−	c.1	8	0.9 ± 0.08	−
		c.2	8	0.89 ± 0.08	−
		c.3	9	1.05 ± 0.09	−
1	0.45 ± 0.03	1.1	5	0.48 ± 0.04	1.14
		1.2	7	0.78 ± 0.07	0.48
		1.3	7	0.78 ± 0.07	0.49
		1.4	7	0.76 ± 0.07	0.54
		1.5	7	0.74 ± 0.07	0.58
2	0.44 ± 0.03	2.1	3	0.2 ± 0.02	1.81
		2.2	6	0.6 ± 0.05	0.92
3	0.05 ± 0.003	3.1	8	0.93 ± 0.08	1.32
		3.2	7	0.74 ± 0.07	4.92

Figure 7. Rope 3 data. Top: acceleration magnitude (solid) and peaks (asterisk). Middle: fall height profile (solid). Bottom: single-event damage (bar) and cumulative damage (dot), both normalized with respect to μ.

unity and a low impact force. This fact justifies why the simpler purely elastic fatigue model can be used to evaluate rope damage. However, plastic behavior could be easily adopted. An indication to the user that plastic deformation has taken place could be relevant as a warning about the intensity of the last fall and the remaining number of falls to failure.

For Ropes 1 and 2, the relatively large number of falls (21) leads to μ-normalized cumulative damages of 0.454 and 0.441, respectively. Conversely, Rope 3 was stressed in only three events for a total damage of 0.053.

The implementation and validation of Leuthäusser's approach on the control rope allowed the determination of the rope damage after each drop test, as seen in Fig. 8. The obtained fatigue model suits the behavior of the field-conditioned ropes because their residual life after the critical number of falls is always less than one.
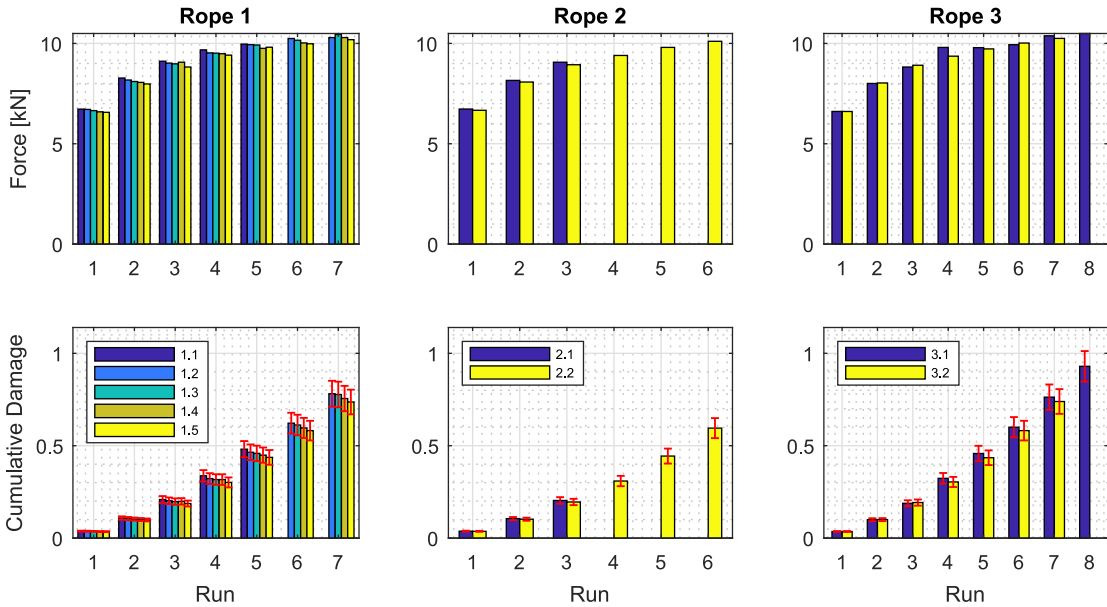
Figure 8. Measured impact force (top) and calculated cumulative damage (bottom) for the climbers' segmented ropes from UIAA tests. Data are plotted for $0 < n \leq n^*$. Failure occurs at $n = n^* + 1$. Cumulative damage error bars are also displayed.

From Table 2, it is seen that Rope 1 requires a lower amount of falls to reach the critical number n^* when compared to the control rope. This particularity also translates into a lower cumulative damage calculated from the drop test results. Furthermore, the rope sample attached to the climber exhibits larger wear than the remaining segments. To accomplish unitary damage, $\mu = 1.14$ is required for the first segment and $0.48 \leq \mu \leq 0.58$ for the others. This value is well above the one used for the UIAA tests ($\mu = 0.09$), which suggests that, on average, the rope is subject to varied and more demanding contact stress conditions when used in the field. However, the attained impact loads are significantly lower in the field when compared to the UIAA tests. This leads to a fairly contained damage of the rope during field conditioning.

Rope 2 exhibits a similar condition to Rope 1. It attains similar damage during field tests and its portion closer to the climber shows increased cumulative damage. However, this damage process seems much faster and larger μ coefficients were necessary to fit the results with the cumulative damage model. According to the user, Rope 2 was exposed to salty and moist environments. Research in this context has demonstrated that humidity has a negative influence on the load-cycle capability of a mountaineering

rope.[15] For marine ropes, Beltran and Williamson state that the failure of a rope element is a complicated process that could depend on a variety of factors, one of them being the environment interaction.[19]

Finally, Rope 3 was used for a very limited number of falls, and hence, the field damage results are not a reliable indicator. The first portion of the rope shows less damage than the second. Also, the calculated μ coefficients are very different because they have to compensate for the inaccuracy of a very small number.

Conclusions

The present study explored the feasibility of estimating the fatigue damage of a climbing rope due to fall events. This estimate is based on the determination of the impact force, which is evaluated from the measurement of the acceleration by means of a wearable device. This information was subsequently correlated with a known rope fatigue characteristic from literature. The obtained results show that the lifespan of the rope can be monitored in real time. Furthermore, experimental data confirmed that the end portion of the rope attached to the climber is prone to greater wear than the rest of the rope.

Moreover, the present research sheds light on the importance of assessing the contact between the rope and the runners when used in the field. In particular, the damage parameter μ varies significantly between field conditioning and UIAA tests. Further dedicated experiments in the field are required to produce reliable μ parameters that suit the behavior in such conditions.

Declaration of conflicting interests

The author(s) declared no potential conflicts of interest with respect to the research, authorship, and/or publication of this article.

Funding

References

1. Blackford JR. Materials in mountaineering. In: Jenkins M (ed) *Materials in Sports Equipment*. Cambridge, England: Woodhead Publishing, 2003, pp. 279–325.
2. DIN EN 566:2007. Mountaineering Equipment–Slings–Safety Requirements and Test Methods.
3. DIN EN 892:2012. Mountaineering Equipment–Dynamic Mountaineering Ropes–Safety Requirements and Test Methods.

4. DIN EN 12275:2013. Mountaineering Equipment–Connectors–Safety Requirements and Test Methods.

5. Centro Ricerche Attrezzature Speleo-alpinistiche e Canyoning (CRASC). Le forze nella progressione, usura materiali e attrezzi fragili. CENS Sigillo, Italy, 2010. URL: http://www.speleocrasc.it/files/Forze-progressione-,-usura-e-fragilita.pdf

6. Manes A, Bedogni V and Rogora D. An experimental methodology for the assessment of climbing devices actual strength. In: *Proceedings of the 15th Conference on Experimental Mechanics*, Porto, Portugal, 2012.

7. Blair KB, Custer DR, Graham JM and Okal MH. Analysis of fatigue failure in D-shaped karabiners. *Sports Eng* 2005; 8: 107–113.

8. May M, Furlan S, Mohrmann H and Ganzenmüller GC. To replace or not to replace? – An investigation into the residual strength of damaged rock climbing safety equipment. *Eng Fail An* 2016; 60: 9–19.

9. Bett J. Analysis of Rock Climbing Falls with Different Rope Paths. Technical Paper, University of Strathclyde, Glasgow, UK, 2013.

10. Manin L, Mahfoudh J, Richard M and Jauffres D. Modeling the Climber Fall Arrest Dynamics. In: *Proceedings of the 2005 ASME International Design Engineering Technical Conferences*, Long Beach, CA, USA, 2005.

11. Manin L, Richard M, Brabant JD and Bissuel M. Rock climbing belay device analysis, experiments and modeling. In: Moritz EF and Haake S (eds) *The Engineering of Sport 6*. New York, NY: Springer, 2006, pp. 69–74.

12. Ernst B and Vogel W. Determination of the redistribution shock load in climbing double rope systems. *Eng Fail An* 2009; 16(3): 751–64.

13. Phillips A, Vogwell J and Bramley A. Forces generated in a climbing rope during a fall. In: Moritz EF and Haake S (eds) *The Engineering of Sport 6*. New York, NY: Springer, 2006, pp. 63–68.

14. Nikonov A, Saprunov I, Zupančič B and Emri I. Influence of moisture on functional properties of climbing ropes. *Int J Impact Eng* 2011; 38(11): 900–909.

15. Spierings AB, Henkel O and Schmid M. Water absorption and the effects of moisture on the dynamic properties of synthetic mountaineering ropes. *Int J Impact Eng* 2007; 34(2): 205—215.

16. Schubert P. About ageing of climbing ropes. *Proceedings of International Moutaineering and Climbing Federation* 2000; 3: 12–13.

17. Mandell JF. Modeling of Marine Rope Fatigue Behavior. *Text Res J* 1987; 57(6): 318–330.

18. Kenney MC, Mandell JF and McGarry FJ. Fatigue behaviour of synthetic fibres, yarns, and ropes. *J Mater Sci* 1985; 20(6): 2045–2059.

19. Beltran JF and Williamson EB. Degradation of rope properties under increasing monotonic load. *Ocean Eng* 2005; 32(7): 826–844.

20. Johnson C and Klonowski C. *Effects of Abrasive Particles on the Projected Fatigue Life of Nylon Climbing Rope*. BS Thesis, California Polytechnic State University, San Luis Obispo, CA, 2012.

21. Pavier M. Experimental and theoretical simulations of climbing falls. *Sports Eng* 1998; 1: 79—91.

22. Leuthäusser U. The physics of a climbing rope under a heavy dynamic load. *Proc IMechE Part P: J Sports Engineering and Technology* 2017; 231(2): 125—135.

23. Leuthäusser U. The fracture of a climbing rope: a phenomenological approach. *Proc IMechE Part P: J Sports Engineering and Technology* 2019; 233(2): 193—201.

24. Tonoli A, Galluzzi R, Zenerino EC and Boero D. Fall identification in rock climbing using wearable device. *Proc IMechE Part P: J Sports Engineering and Technology* 2016; 230(3): 171–179.

25. Bonfitto A, Tonoli A, Feraco S, Zenerino EC and Galluzzi R. Pattern recognition neural classifier for fall detection in rock climbing. *Proc IMechE Part P: J Sports Engineering and Technology* 2019; 233(4): 478–488.

26. UIAA Safety Standard 101:2018. Dynamic Ropes.